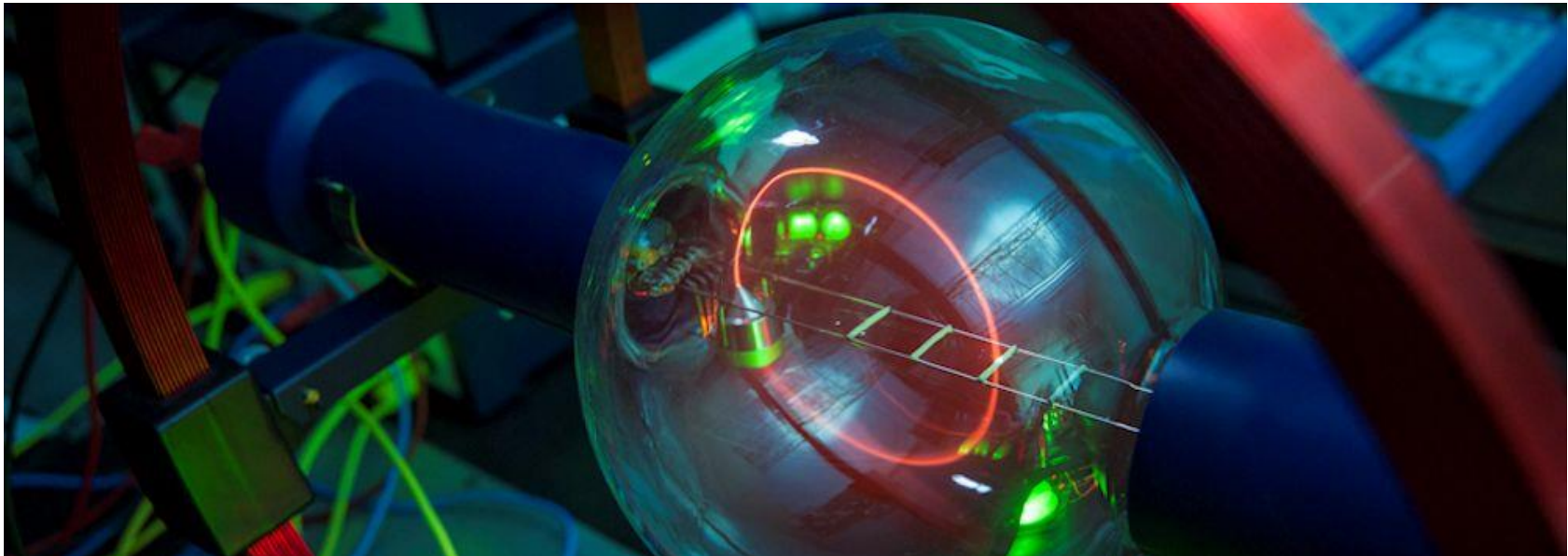


Condensed Matter Physics

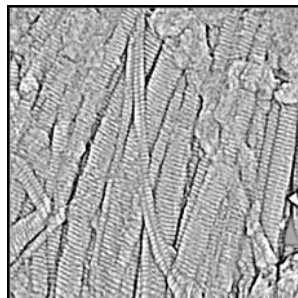
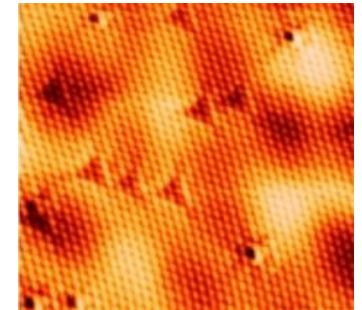
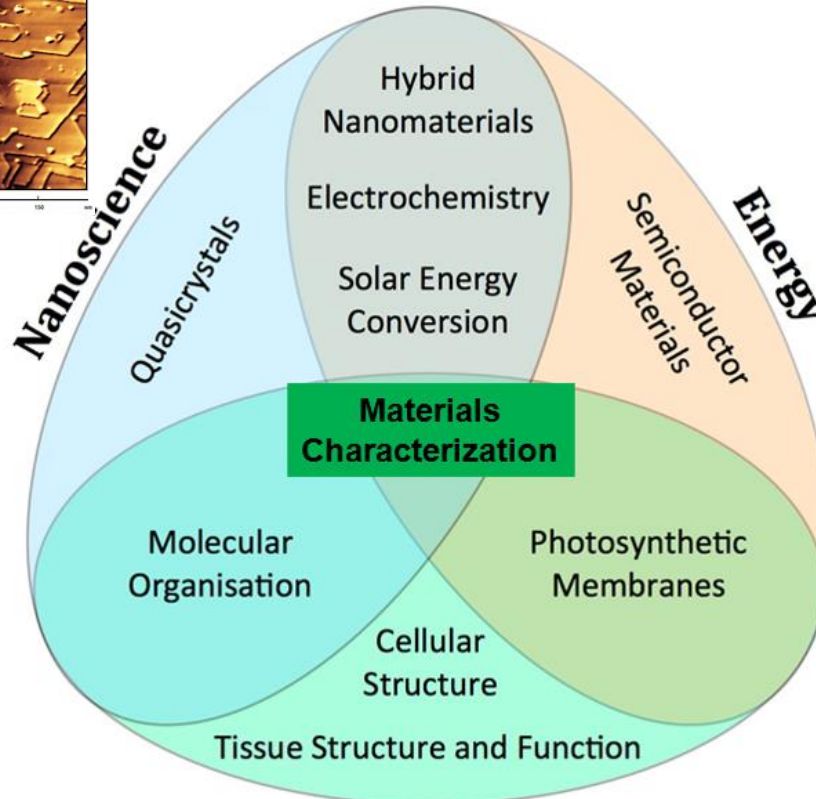
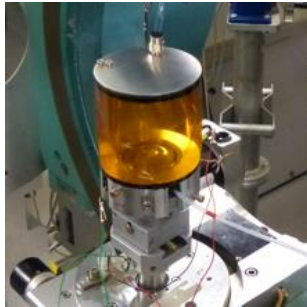
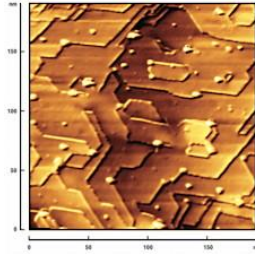
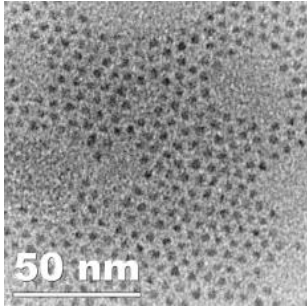
“Discipline that treats the thermal, elastic, electrical, magnetic, and optical properties of solid and liquid substances”
Encyclopaedia Britannica

- So, things we instinctively understand: crystals, amorphous solids, films, metals, liquids...
- But also: liquid- and quasicrystals, superconductors, magnets, glasses, soft materials...
- Main idea: “A system of many interacting parts can have properties that the parts do not have”

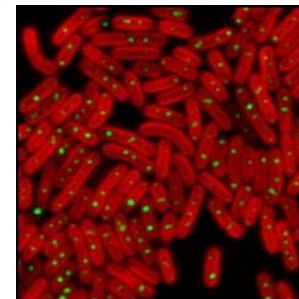


CMP Research Areas at University of Liverpool

<https://www.liverpool.ac.uk/physics/research/condensed-matter-physics/>



Biophysics



CMP Academic staff at University of Liverpool

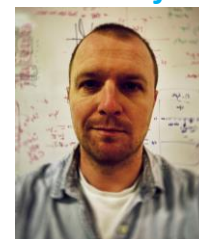
Yvonne Gründer



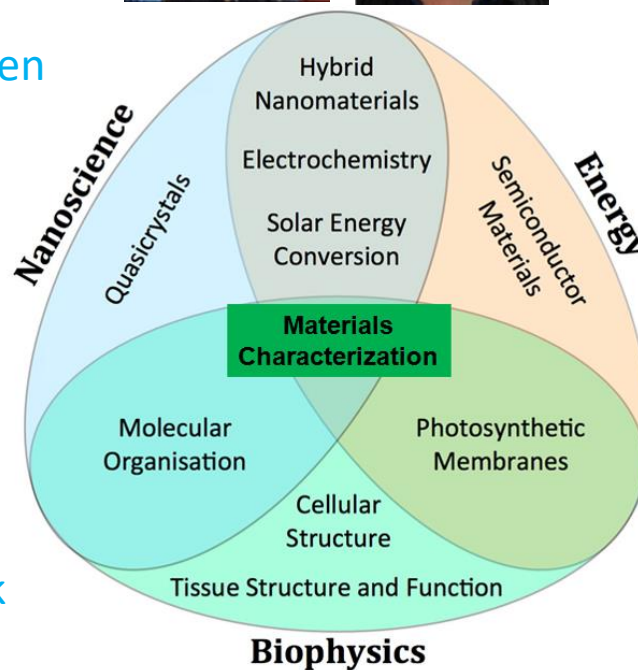
Chris Lucas



Jon Major Ken Durose



Hem Sharma Liam O'Brien



Tim Veal



Jon Alaria

Ronan McArthur Vin Dhanak



Brianna Heazlewood Frank Jaeckel



Joe Forth

Peter Weightman



David Martin

Unraveling the Charge Distribution at the Metal-Electrolyte Interface Coupling in Situ Surface Resonant X-Ray Diffraction with Ab Initio Calculations

Yvonne Soldo-Olivier,* Eric Sibert, Maurizio De Santis, Yves Joly, and Yvonne Gründer



Cite This: *ACS Catal.* 2022, 12, 2375–2380



Read Online

ACCESS |



Metrics & More



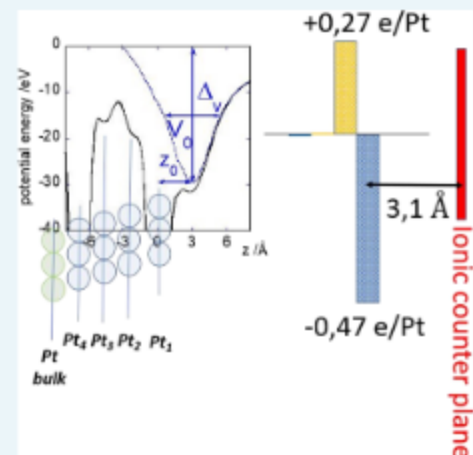
Article Recommendations



Supporting Information

ABSTRACT: The comprehension of the mechanisms underlying the charge distribution at the electrochemical interface is a fundamental step in sight of the performance of catalytic materials. Several techniques allow the atomic structure of the metal surface to be characterized, while no experimental method enables to obtain the charge distribution at the catalyst surface and in the electrolyte in the interfacial region. Combining experimental and *ab initio* calculations, we succeeded in quantitatively describing the charge distribution at the electrochemical interface of the archetypal system Pt(111) in an acidic medium. In our approach, we couple *in situ* surface resonant X-ray diffraction, a site-sensitive experimental technique probing both the atomic and the electronic surface structures, with *ab initio* calculations, recently implemented to describe the Helmholtz double layer formed at the metal-solution interface. In the potential region in between the hydrogen desorption and the (bi)sulfate adsorption, we could determine the charge distribution on each of the metal surface layers and the distance separating the metal from the oppositely charged disordered ionic plane. We could reveal the presence of an electric dipole over the two outermost platinum layers. Our results demonstrate the potential of this original approach to unveil the electronic densities at the electrochemical interfaces, a challenging topic for the understanding of electrochemical reactivity.

KEYWORDS: charge at the electrochemical interface, *in situ* surface resonant XRD, *ab initio* calculations, DFT, platinum single crystal



Sb₂S₃ Thin-Film Solar Cells Fabricated from an Antimony Ethyl Xanthate Based Precursor in Air

Jako S. Eensalu,* Sreekanth Mandati, Christopher H. Don, Harry Finch, Vinod R. Dhanak, Jonathan D. Major, Raitis Grzibovskis, Aile Tamm, Peeter Ritslaid, Raavo Josepson, Tanel Käämbre, Aivars Vembris, Nicolae Spalatu, Malle Krunks,* and Ilona Oja Acik



Cite This: <https://doi.org/10.1021/acsami.3c08547>



Read Online

ACCESS |



Metrics & More



Article Recommendations

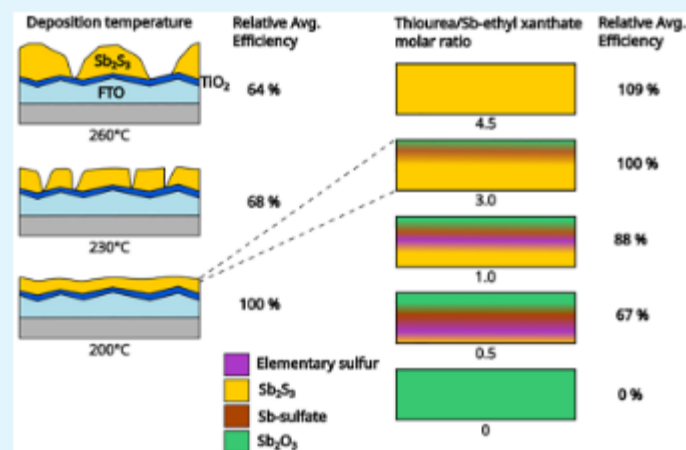


Supporting Information


ABSTRACT: The rapidly expanding demand for photovoltaics (PVs) requires stable, quick, and easy to manufacture solar cells based on socioeconomically and ecologically viable earth-abundant resources. Sb₂S₃ has been a potential candidate for solar PVs and the efficiency of planar Sb₂S₃ thin-film solar cells has witnessed a reasonable rise from 5.77% in 2014 to 8% in 2022. Herein, the aim is to bring new insight into Sb₂S₃ solar cell research by investigating how the bulk and surface properties of the Sb₂S₃ absorber and the current–voltage and deep-level defect characteristics of solar cells based on these films are affected by the ultrasonic spray pyrolysis deposition temperature and the molar ratio of thiourea to SbEX in solution. The properties of the Sb₂S₃ absorber are characterized by bulk- and surface-sensitive methods. Solar cells are characterized by temperature-dependent current–voltage, external quantum efficiency, and deep-level transient spectroscopy measurements. In this paper, the first thin-film solar cells based on a planar Sb₂S₃ absorber grown from antimony ethyl xanthate (SbEX) by ultrasonic spray pyrolysis in air are demonstrated. Devices based on the Sb₂S₃ absorber grown at 200 °C, especially from a solution of thiourea and SbEX in a molar ratio of 4.5, perform the best by virtue of suppressed surface oxidation of Sb₂S₃, favorable band alignment, Sb-vacancy concentration, a continuous film morphology, and a suitable film thickness of 75 nm, achieving up to 4.1% power conversion efficiency, which is the best efficiency to date for planar Sb₂S₃ solar cells grown from xanthate-based precursors. Our findings highlight the importance of developing synthesis conditions to achieve the best solar cell device performance for an Sb₂S₃ absorber layer pertaining to the chosen deposition method, experimental setup, and precursors.

The properties of the Sb₂S₃ absorber are characterized by bulk- and surface-sensitive methods. Solar cells are characterized by temperature-dependent current–voltage, external quantum efficiency, and deep-level transient spectroscopy measurements. In this paper, the first thin-film solar cells based on a planar Sb₂S₃ absorber grown from antimony ethyl xanthate (SbEX) by ultrasonic spray pyrolysis in air are demonstrated. Devices based on the Sb₂S₃ absorber grown at 200 °C, especially from a solution of thiourea and SbEX in a molar ratio of 4.5, perform the best by virtue of suppressed surface oxidation of Sb₂S₃, favorable band alignment, Sb-vacancy concentration, a continuous film morphology, and a suitable film thickness of 75 nm, achieving up to 4.1% power conversion efficiency, which is the best efficiency to date for planar Sb₂S₃ solar cells grown from xanthate-based precursors. Our findings highlight the importance of developing synthesis conditions to achieve the best solar cell device performance for an Sb₂S₃ absorber layer pertaining to the chosen deposition method, experimental setup, and precursors.

KEYWORDS: Antimony sulfide, chemical synthesis, photovoltaics, solar cells, spray pyrolysis, thin films



Entropy-driven order in an array of nanomagnets

Hilal Saglam¹, Ayhan Duzgun², Aikaterini Kargioti¹, Nikhil Harle ³, Xiaoyu Zhang¹,
Nicholas S. Bingham¹, Yuyang Lao⁴, Ian Gilbert^{4,10}, Joseph Sklenar^{4,5}, Justin D. Watts ^{6,7},
Justin Ramberger⁶, Daniel Bromley⁸, Rajesh V. Chopdekar ⁹, Liam O'Brien ⁸, Chris Leighton ⁶,
Cristiano Nisoli ²  and Peter Schiffer ^{1,3,4} 

Long-range ordering is typically associated with a decrease in entropy. Yet, it can also be driven by increasing entropy in certain special cases. Here we demonstrate that artificial spin-ice arrays of single-domain nanomagnets can be designed to produce such entropy-driven order. We focus on the tetris artificial spin-ice structure, a highly frustrated array geometry with a zero-point Pauling entropy, which is formed by selectively creating regular vacancies on the canonical square ice lattice. We probe thermally active tetris artificial spin ice both experimentally and through simulations, measuring the magnetic moments of the individual nanomagnets. We find two-dimensional magnetic ordering in one subset of these moments, which we demonstrate to be induced by disorder (that is, increased entropy) in another subset of the moments. In contrast with other entropy-driven systems, the discrete degrees of freedom in tetris artificial spin ice are binary and are both designable and directly observable at the microscale, and the entropy of the system is precisely calculable in simulations. This example, in which the system's interactions and ground-state entropy are well defined, expands the experimental landscape for the study of entropy-driven ordering.

Growth of pentacene molecules on Tsai-type quasicrystals and related crystal surfaces

Cite as: *J. Vac. Sci. Technol. A* **40**, 013211 (2022); doi: [10.1116/6.0001412](https://doi.org/10.1116/6.0001412)

Submitted: 30 August 2021 · Accepted: 16 November 2021 ·

Published Online: 13 December 2021



View Online



Export Citation



CrossMark

H. R. Sharma,^{1,a)}  S. Coates,²  A. Alofi,¹ and R. McGrath¹ 

AFFILIATIONS

¹Surface Science Research Centre, Department of Physics, University of Liverpool, Liverpool L69 3BX, United Kingdom

²Department of Materials Science and Technology, Tokyo University of Science, Tokyo 125-8585, Japan

Note: This paper is a part of the Special Collection Commemorating the Career of Pat Thiel.

^{a)}Electronic mail: H.R.Sharma@liverpool.ac.uk

ABSTRACT

We present a study of the adsorption of pentacene (Pn) molecules on the high symmetry (fivefold, threefold, and twofold) surfaces of the icosahedral (*i*) Ag–In–Yb quasicrystal. We also compare the results with adsorption of Pn on a surface of a periodic crystal related to this quasicrystal, the (111) surface of the Au–Al–Tb 1/1 approximant. Scanning tunneling microscopy reveals that Pn molecules on the quasicrystal surfaces are aligned along the high symmetry directions of the substrates and selectively adsorb on Yb atoms and thus exhibit quasicrystalline order. Pn molecules on the Au–Al–Tb approximant surface also preferably adopt Tb sites. The behavior of selective adsorption can be understood in terms of the geometry and electronic properties of the adsorbate and substrate. The Yb–Yb (Tb–Tb) separations are comparable to the C–C or H–H distances in a Pn molecule. Pn is an electron donor, whereas the unoccupied electronic states of the substrate are dominated by the rare earth atoms, suggesting that there is an electronic transfer between the Pn molecules and Yb (Tb) atoms.

© 2021 Author(s). All article content, except where otherwise noted, is licensed under a Creative Commons Attribution (CC BY) license (<http://creativecommons.org/licenses/by/4.0/>). <https://doi.org/10.1116/6.0001412>

Fluorine-Rich Oxyfluoride Spinel-like $\text{Li}_{1.25}\text{Ni}_{0.625}\text{Mn}_{1.125}\text{O}_3\text{F}$ Utilizing Redox-Active Ni and Mn for High Capacity and Improved Cyclability

Hong Cai, Ruiyong Chen, Mounib Bahri, Cara J. Hawkins, Manel Sonni, Luke M. Daniels, Jungwoo Lim, Jae A. Evans, Marco Zanella, Leanne A. H. Jones, Troy D. Manning, Tim D. Veal, Laurence J. Hardwick, Matthew S. Dyer, Nigel D. Browning, John B. Claridge, and Matthew J. Rosseinsky*



Cite This: *ACS Materials Lett.* 2023, 5, 527–535



Read Online

ACCESS |



Metrics & More

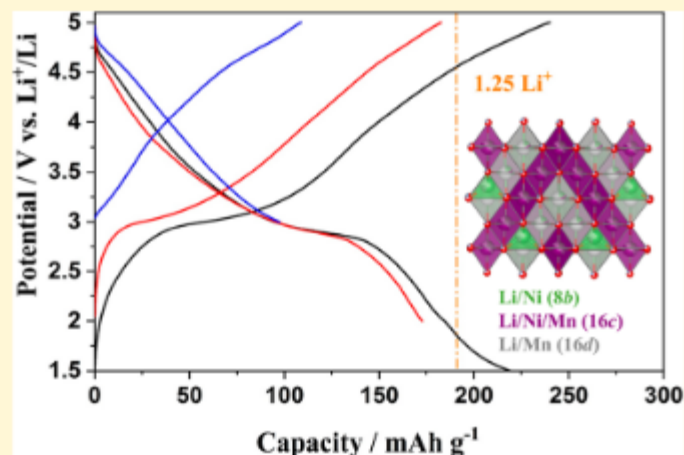


Article Recommendations



Supporting Information

ABSTRACT: Extending the accessible capacity and cyclability is of central interest for cathode materials for Li-ion batteries. Here, we report the successful synthesis of a new spinel-like $\text{Li}_{1.25}\text{Ni}_{0.625}\text{Mn}_{1.125}\text{O}_3\text{F}$ ($Fd\bar{3}m$) oxyfluoride with significant cation disorder characterized by combined refinement of X-ray and neutron diffraction data. $\text{Li}_{1.25}\text{Ni}_{0.625}\text{Mn}_{1.125}\text{O}_3\text{F}$ utilizes redox reactions of both Ni and Mn, accessing capacities of 225 (i.e., 1.46 Li^+ capacity) and 285 mAh g^{-1} (i.e., 1.85 Li^+ capacity) at 25 and 40 °C, respectively, through intercalation of additional Li^+ into the lattice. Moreover, compared to lithium transition metal disordered rocksalt or spinel-like oxyfluorides previously reported, $\text{Li}_{1.25}\text{Ni}_{0.625}\text{Mn}_{1.125}\text{O}_3\text{F}$ shows significantly improved cycling stability. Ex situ compositional, structural, and spectroscopic analyses of samples at different states of charge/discharge confirm a single-phase intercalation reaction and high structural integrity over cycling.



Charge Transfer Reactions between Water Isotopologues and Kr^+ ions

Andriana Tsikritea, Jake A. Diprose, Jérôme Loreau, and Brianna R. Heazlewood*



Cite This: *ACS Phys. Chem Au* 2022, 2, 199–205



Read Online

ACCESS |



Metrics & More



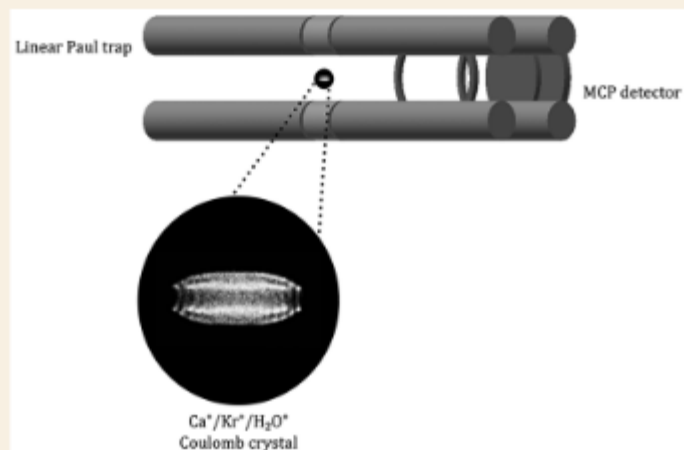
Article Recommendations



Supporting Information

ABSTRACT: Astrochemical models often adopt capture theories to predict the behavior of experimentally unmeasured ion–molecule reactions. Here, reaction rate coefficients are reported for the charge transfer reactions of H_2O and D_2O molecules with cold, trapped Kr^+ ions. Classical capture theory predictions are found to be in excellent agreement with the experimental findings. A crossing point identified between the reactant and product potential energy surfaces, constructed from high-level *ab initio* calculations, further supports a capture-driven mechanism of charge transfer. However, ion–molecule reactions do not always agree with predictions from capture theory models. The appropriateness of using capture theory-based models in the absence of detailed experimental or theoretical studies is discussed, alongside an analysis of why capture theory is appropriate for describing the likelihood of charge transfer between Kr^+ and the two water isotopologues.

KEYWORDS: *Coulomb crystals, reaction kinetics, ab initio calculations, capture theory models, astrochemistry*



Metric-based analysis of FTIR data to discriminate tissue types in oral cancer†

Barnaby G. Ellis,^a James Ingham,^{ID}^a Conor A. Whitley,^a Safaa Al Jedani,^a
Philip J. Gunning,^{ID}^b Peter Gardner,^{ID}^c Richard J. Shaw,^{ID}^{b,d} Steve D. Barrett,^{ID}^a
Asterios Triantafyllou,^{ID}^e Janet M. Risk,^{ID}^b Caroline I. Smith,^{ID}^a and
Peter Weightman,^{ID}^{*a}

A machine learning algorithm (MLA) has predicted the prognosis of oral potentially malignant lesions and discriminated between lymph node tissue and metastatic oral squamous cell carcinoma (OSCC). The MLA analyses metrics, which are ratios of Fourier transform infrared absorbances, and identifies key wavenumbers that can be associated with molecular biomarkers. The wider efficacy of the MLA is now shown in the more complex primary OSCC tumour setting, where it is able to identify seven types of tissue. Three epithelial and four non-epithelial tissue types were discriminated from each other with sensitivities between 82% and 96% and specificities between 90% and 99%. The wavenumbers involved in the five best discriminating metrics for each tissue type were tightly grouped, indicating that small changes in the spectral profiles of the different tissue types are important. The number of samples used in this study was small, but the information will provide a basis for further, larger investigations.

Harnessing liquid-in-liquid printing and micropatterned substrates to fabricate 3-dimensional all-liquid fluidic devices

[Wenqian Feng](#), [Yu Chai](#), [Joe Forth](#), [Paul D. Ashby](#), [Thomas P. Russell](#) & [Brett A. Helms](#) 

Nature Communications **10**, Article number: 1095 (2019) | [Cite this article](#)

9766 Accesses | **92** Citations | **139** Altmetric | [Metrics](#)

Abstract

Systems comprised of immiscible liquids held in non-equilibrium shapes by the interfacial assembly and jamming of nanoparticle–polymer surfactants have significant potential to advance catalysis, chemical separations, energy storage and conversion. Spatially directing functionality within them and coupling processes in both phases remains a challenge. Here, we exploit nanoclay–polymer surfactant assemblies at an oil–water interface to produce a semi-permeable membrane between the liquids, and from them all-liquid fluidic devices with bespoke properties. Flow channels are fabricated using micropatterned 2D substrates and liquid-in-liquid 3D printing. The anionic walls of the device can be functionalized with cationic small molecules, enzymes, and colloidal nanocrystal catalysts. Multi-step chemical transformations can be conducted within the channels under flow, as can selective mass transport across the liquid–liquid interface for in-line separations. These all-liquid systems become automated using pumps, detectors, and control systems, revealing a latent ability for chemical logic and learning.

Stephenson Institute for Renewable Energy (SIRE)



Stephenson Institute for Renewable Energy (SIRE)

Nanomaterials Characterisation Laboratory (NCL) ran by Vin Dhanak - three UHV stations providing techniques such as XPS, UPS, LEED I-V, STM and IPES

Veal Group Facilities ran by Tim Veal - Fourier transform infrared/visible spectrometer, Electrochemical capacitance-voltage profiler, Hall effect system, Seebeck/thermopower measurement system

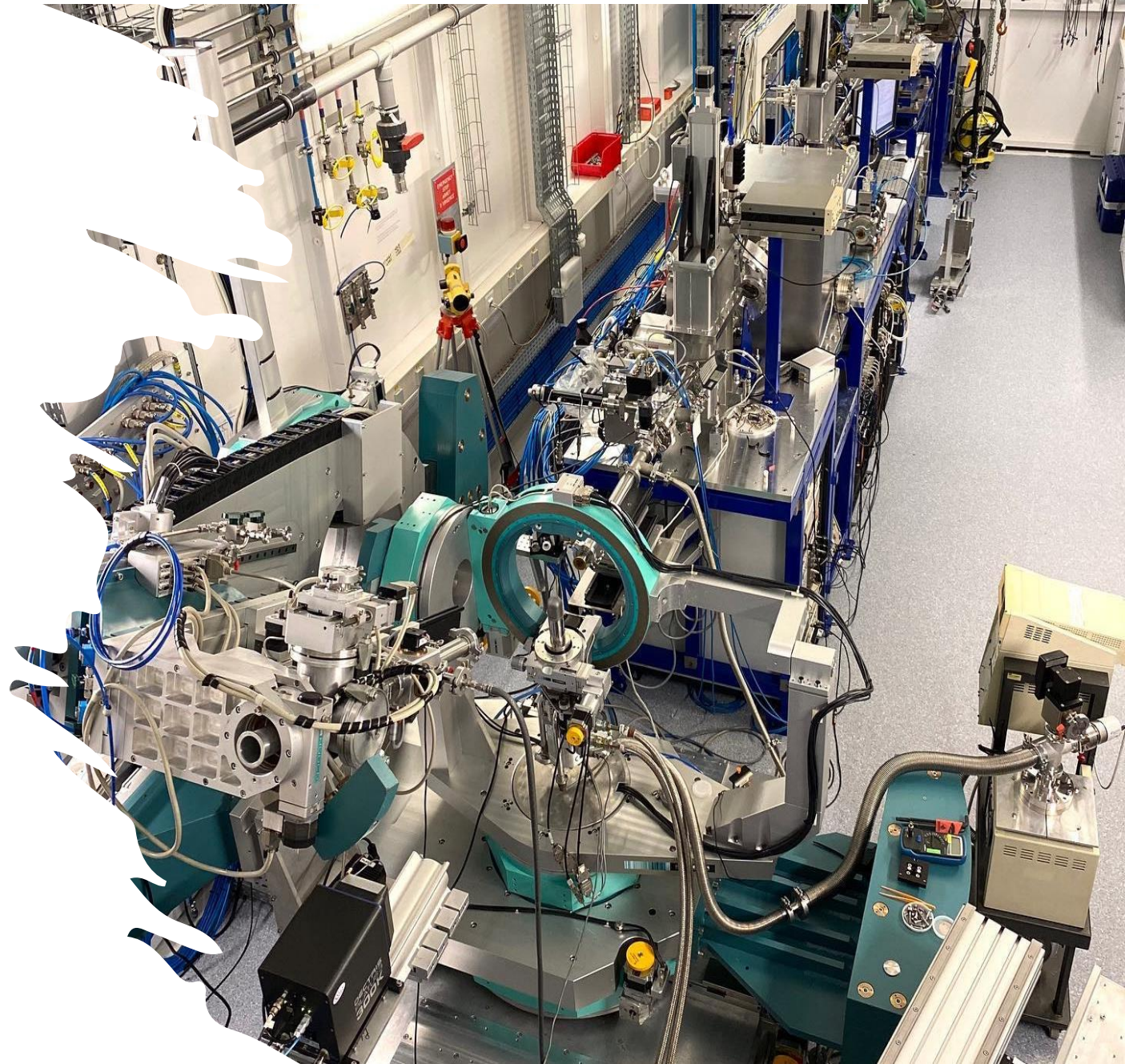
X-ray facility ran by Jonathan Alaria – available as part of the Shared Research Facility (SRF), advanced structural characterisation

Laue System ran by Ken Durose – X-ray diffractometer with excellent control over the crystal positioning



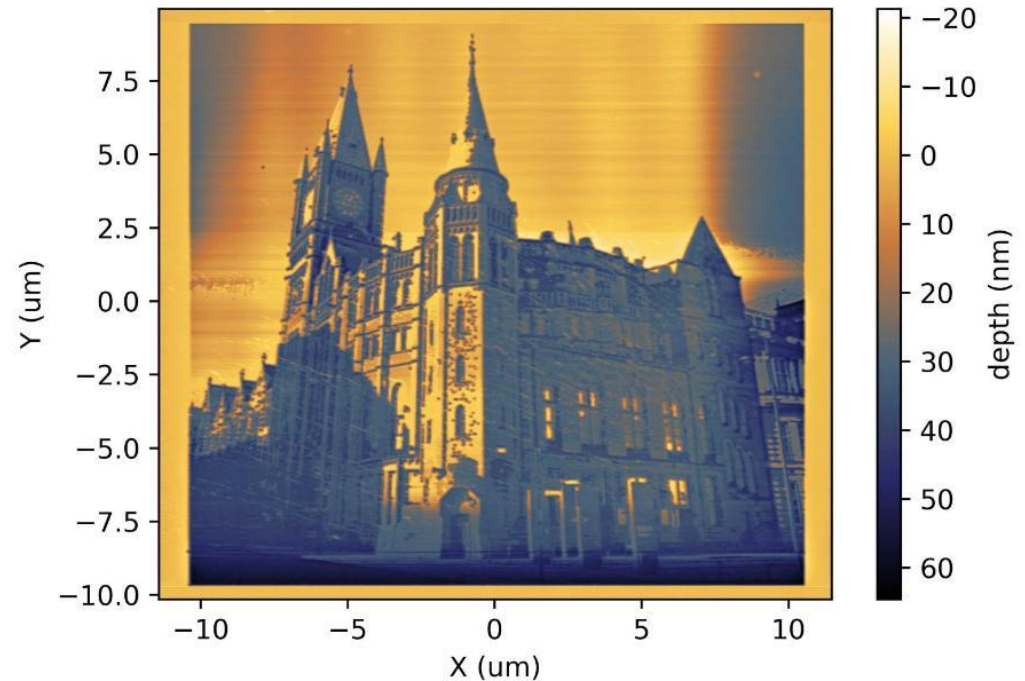
XMaS: The UK X-ray Materials Science facility at the ESRF in Grenoble

- Ran by Chris Lucas and Yvonne Gründer
- Diffraction
- Resonant Elastic X-ray scattering
- Grazing Incidence (reflectivity, diffraction, etc.)
- Spectroscopy
- Small Angle Scattering ($>0.01 \text{ \AA}^{-1}$)



Nanolithography-nanofrazor

- Ran by Liam O'Brien in collaboration with Chemistry
- Patterning (etching, depositing, writing, printing, etc.) of nanometer-scale structures on various materials and immediate scanning of the product
- Part of the SRF



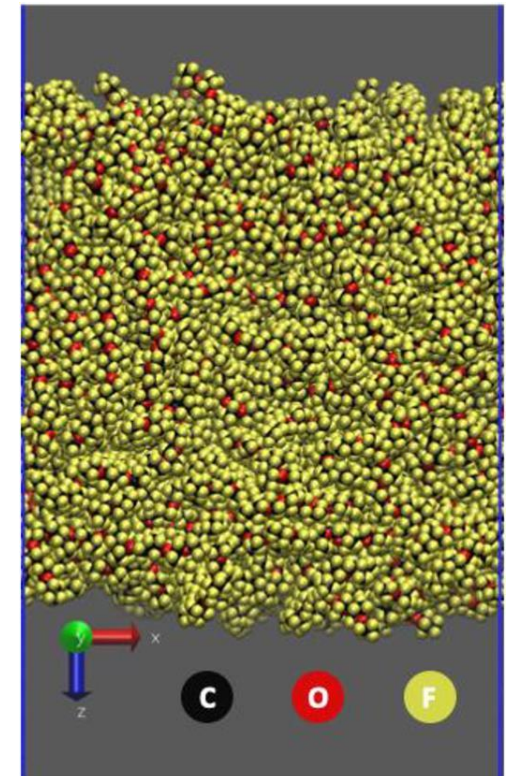
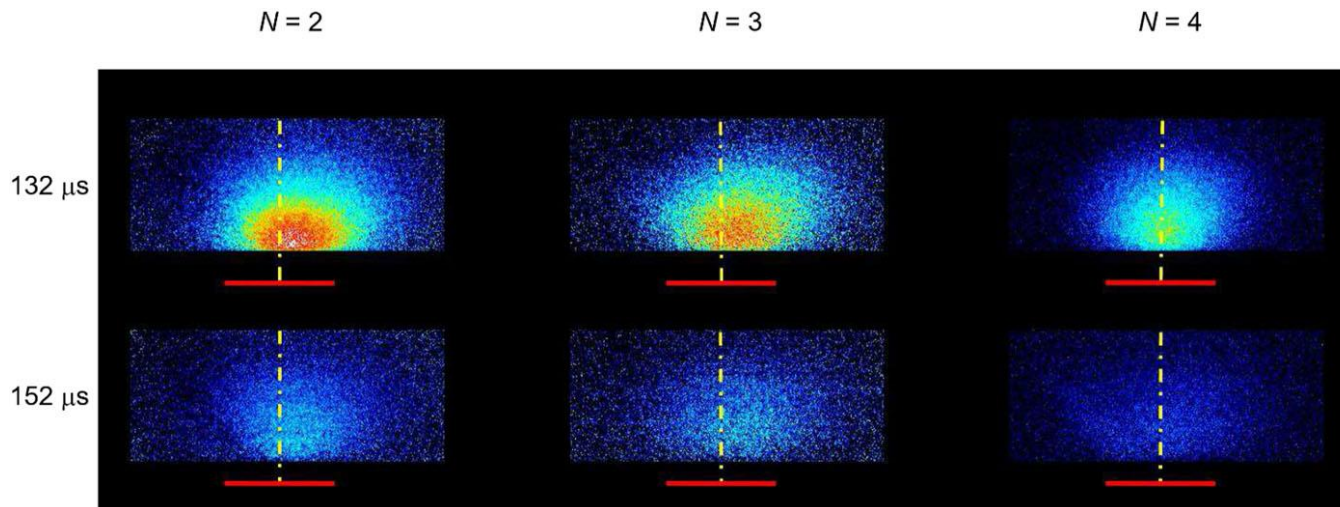
Shared Research Facilities (SRF)

“The Faculty of Science and Engineering has invested in the provision of our Shared Research Facilities in order to facilitate world class research. Our facilities, equipment, and staff are here to support research and teaching for both internal users and external partners and we offer flexible and efficient access to suit a variety of needs.”

- Range of instruments/facilities available to book
- Includes instruments ran by CMP cluster members:
 - X-ray Diffraction Facility ran by Jonathan Alaria
 - Nanolithography Suite ran by Liam O’Brien
- More info: <https://www.liverpool.ac.uk/science-and-engineering/shared-research-facilities/>

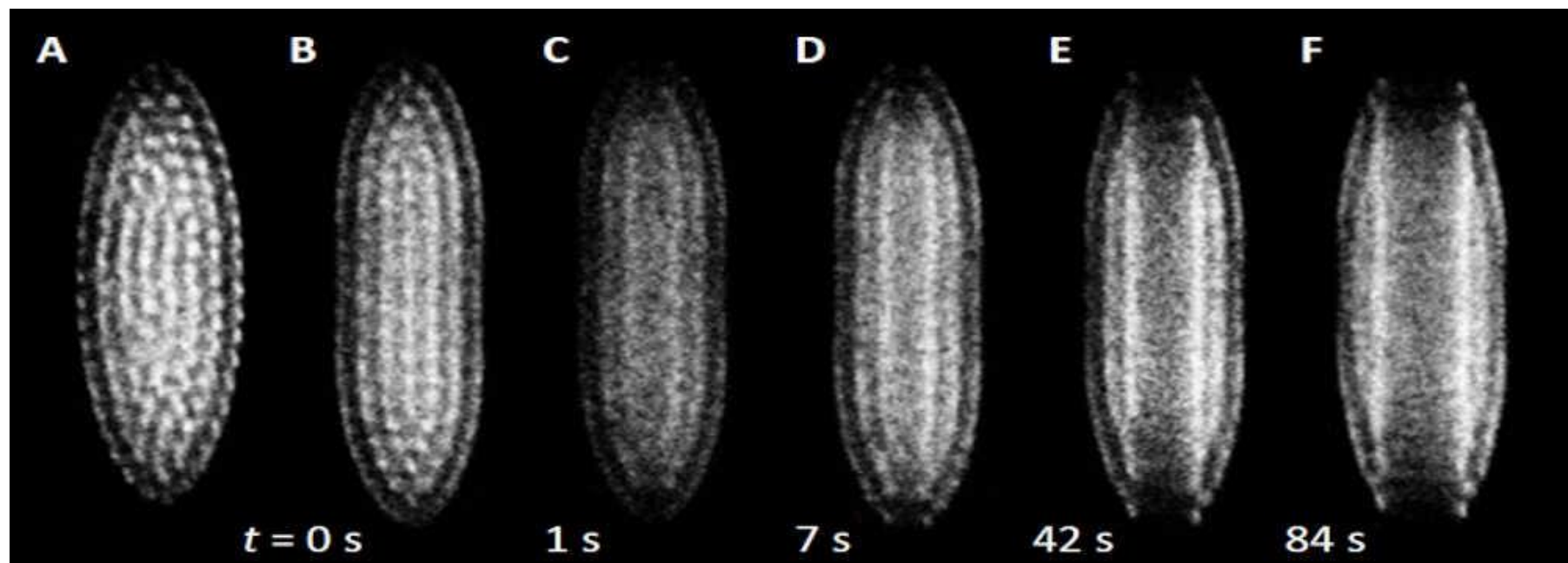
My experience as part of the CMP cluster

- Relatively new, joined as PDRA in October 2022
- PhD in Physical Chemistry, so distinctively not a physicist
- However, researched interactions on the gas-liquid surfaces by studying OH scattering from long-chain hydrocarbons
- So, I guess some CMP experience
- <https://pubs.aip.org/aip/jcp/article/151/5/054201/198655/Real-space-laser-induced-fluorescence-imaging>



My experience as part of the CMP cluster

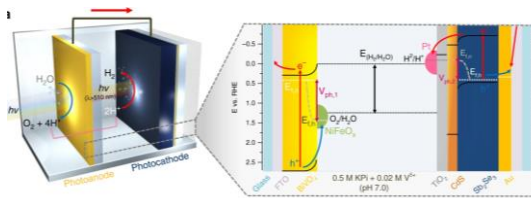
- Currently working for Brianna Heazlewood on reaction dynamics of ion-radical reactions
- Research utilises molecular beam techniques and ion trapping
- Trapping ions using electric fields and laser cooling to form Coulomb crystals
- “Crystals” make it sound very CMP-like, but in fact they are very long range, with distances of tens of micrometres between constituent ions – not quite “condensed”



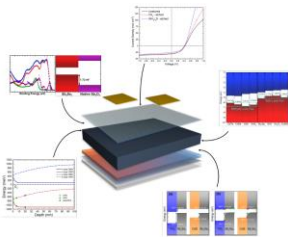
My experience as part of the CMP cluster

- Therefore, CMP is an entirely new world to me, everything is shiny and exciting
- Doing this presentation really showed me the diversity of research topics that the simple label of “CMP” encompasses
- Also, very applicable-to-real-life research, compared to research done previously by me

Solar Cells and Photocatalyst



Benchmark performance of low-cost Sb_2Se_3 photocathodes for unassisted solar overall water splitting, *Nature Communications* 11, 861 (2020)



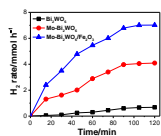
Band alignments and interfaces in Antimony Selenide Solar Cells

Single Crystal Growth



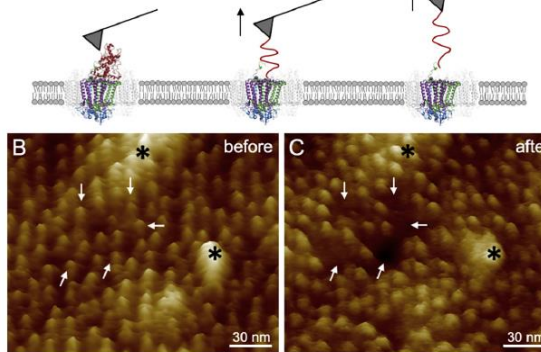
Antimony selenide

Nano heterostructures for photocatalysis



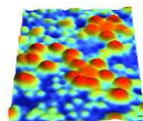
Mo-doped $\text{Bi}_2\text{WO}_6/\text{Fe}_2\text{O}_3$

Light-harvesting in Photosynthetic Bacteria

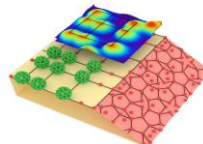


Investigating light-harvesting complexes in photosynthetic bacteria using atomic force microscopy

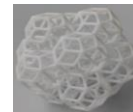
Multiscale Quasicrystals



Quasicrystalline Pb
Nature Communications 4, 2715 (2013).

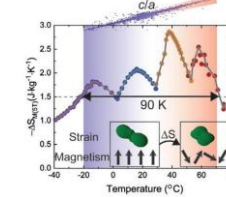


C_{60} adsorbs atop Fe/Mn atoms forming unique quasicrystalline structures such as Penrose tiling and Fibonacci square
Nature Communications 9, 3435 (2018)



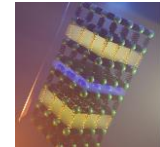
3D printed QC structure (35 mm diameter)

Magnetic Refrigeration



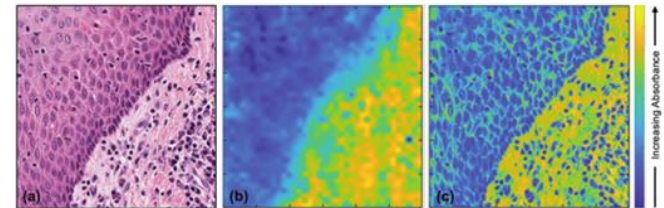
Combining Experiment and Machine Learning to Make a Cool Choice, *Adv. Funct. Mater.* 2021, 31, 2100108

Inorganic Material with Low Thermal Conductivity



Using the right chemistry, it is possible to combine two different atomic arrangement (yellow and blue slabs) that provide mechanisms to slow down the motion of heat through a solid. *Science* 373, 1017 (2021)

Cancer Diagnosis



(a) H&E stained image of a tissue biopsy, (b) corresponding Fourier transform IR image at 1242 cm^{-1} and (c) the image formed by fusing (a) and (b). *Analyst* 146 5848 (2021)